China Petroleum Processing and Petrochemical Technology

Catalyst Research Volume 23, Issue 2, September 2023 Pp. 1262-1278

LAPLACE TRANSFORM APPROACH FOR AN IMPULSIVELY MOVING PLATE ON A COPPER-WATER BASED MAGNETO-NANOFLUID WITH ISOTHERMAL AND RAMPED TEMPERATURE.

M. R. Mishra
Department of Mathematics, OP Jindal University, Raigarh, India

D. Samal
Department of Mathematics, OP Jindal University, Raigarh, India

S. Singh
Department of Mathematics, OP Jindal University, Raigarh, India

***Corresponding Author**: M. R. Mishra
*Department of Mathematics, OP Jindal University, Raigarh, India

Abstract
The intention of the current research is to investigate how heat absorption affects the transient magneto-nanofluid free convective boundary layer flow of an electrically conducting, viscous, and incompressible over an impulsively moving vertical ramping temperature plate. The TiO_2, Al_2O_3, and Cu nanoparticles added to the water-based nanofluids are taken into consideration. The governing model is analytically resolved by using the Laplace transform approach. For both the cases of ramped and isothermal settings, the expressions for nanofluid velocity, temperature, skin friction, and Nusselt number have been found. The effects of physical parameters on the nanofluid velocity and are demonstrated by many graphs and tables.
Keywords: Hydromagnetic flow, Free convection, Heat absorption, isothermal and Ramped temperature

U	component of nanofluid velocity in x'-direction
α'	temperature of the nanofluid
ρ_{nf}	density of the nanofluid
μ_{nf}	dynamic viscosity of the nanofluid
σ_{nf}	electrical conductivity of the nanofluid
g	acceleration due to gravity
β_{nf}	thermal expansion coefficient of the nanofluid
$\left(\rho c_p\right)_{nf}$	heat capacitance of the nanofluid
Q_0	heat absorption coefficient
k_{nf}	thermal conductivity of the nanofluid

ϕ volume fraction of nanoparticle
ρ_f density of the base fluid
ρ_s density of the nanoparticle
μ_f viscosity of the base fluid
β_f thermal expansion coefficient of the base fluid
β_s thermal expansion coefficient of the nanoparticle
$(\rho c_p)_f$ heat capacitance of the base fluid
$(\rho c_p)_s$ heat capacitance of the nanoparticle
σ_f electrical conductivity of the base fluid
σ_s electrical conductivity of the nanoparticle
k_f thermal conductivity of the base fluid
k_s thermal conductivity of the nanoparticles.
M magnetic parameter
Q heat absorption parameter Q
G_r Grash of number
P_r Prandtl number.

1. INTRODUCTION

Numerous researchers have become interested in nanofluid because of widely applied it to various fields and companies. Initially, the Choi [1] term "nanofluid" refers to the suspension of nanoparticles with a diameter of less than 100 nm in a base fluid like water or ethylene glycol. Typically, the basic fluids used in practical applications are lack of sufficient thermal conductivity. As a result, metal nanoparticles with a higher thermal conductivity than the convectional base fluid are mixed in with the fluid to increase its thermal conductivity. Being a mixture of nanoparticles and the base fluid, nanofluids are a revolutionary type of energy transmission fluid, and their unique quality makes them extremely helpful in many heat transfer processes, such as in microelectronics, cars, and other mechanical devices. Choi [1], first who pointed out that the thermal conductivity of base fluid can be improved radically by the uniform dispersion of nano-sized particles into a fluid. This idea attracted a lot of researchers to nanofluids, and numerous studies examining the thermal characteristics of nanofluids have been developed. Keblinski et al. [2] investigate a potential mechanism whereby the uniform suspension of nano-sized particles in the fluid increases the fluid's thermal conductivity. According to the non-homogeneous equilibrium model put forth by Buongiorno [3], the presence of Brownian diffusion and the thermophoretic diffusion effects of nanoparticles can considerably improve the thermal conductivity of a fluid. The remarkable research works by Jang and Choi [4], Daungthongsuk and Wongwises [5], Seyyedi et al. [6], Rashidi et al. [7], Garoosi et al. [8-9], and Malvandi and Ganji

[10-11] have all reported improvements in the thermal conductivity of fluids caused by the suspension of nanoparticles and their applications.

The hydromagnetic nanofluids are recognized to have fascinating importance to various magneto-optical wavelength filters, ink float separation, optical switches and gratings, nonlinear optical materials, etc. They have both the liquid and magnetic characteristics. After that, Sheikholeslami et al. [12–14] revealed the results of their research into the issues with MHD convective flow of nanofluids while taking into account various geometries and configurations. A theoretical analysis of the issue of hydromagnetic flow in a permeable channel filled with nanofluid was conducted by Sheikholeslami and Ganji [15]. They came to the conclusion that the nanofluid velocity boundary layer thickness decreases as a result of rising Reynolds number and nanoparticle volume percent, however it increases when Hartmann number rises. Recently, Hayat et al. [16] investigated the unstable hydromagnetic bidirectional compressive current of nanofluids confined between two parallel walls under the influence of Brownian motion and thermophoresis effects. More recently, Dhanai et al. [17] investigated the effect of thermal slip on the convection current of the hydromagnetic mixture of nanofluids with heat transfer along an inclined cylinder taking into account the effects of heat transfer, Brownian motion and dissipation. viscous. They concluded that an increase in mass transfer parameter leads to an increase in heat transfer rate while it decreases due to thermal slip parameter.

The heat generation /absorption plays an important role on the heat transfer characteristics in the various physical phenomena involved in the industry such as dissociating fluids in packed bed reactors, post accident heat removal, fire and combustion, underground disposal of radioactive waste material, storage of food stuffs, etc. This encouraged many researchers to undertake the investigation of hydromagnetic convective flow over the bodies with different geometries under the influence of heat generation/absorption. Some relevant investigations dealing with the influence of heat generation or absorption have been reported by Acharya and Goldstein [18], Vajravelu and Nayfeh [19], Chamkha [20], Leea *et al*. [21], Sheikh and Abbas [22], Mehmood and Saleem [23], Mondal *et al*. [24] and Nandkyeolyar *et al*. [25]. Hamad and Pop [26] investigated the unsteady free convective nanofluid flow over an oscillatory moving vertical permeable flat plate under the influence of constant heat source and magnetic field in a rotating frame of reference. Chamkha and Aly [27] studied the 2-dimensional steady hydromagnetic free convective boundary-layer nanofluid flow of an incompressible pure base fluid suspended with nanoparticles over semi-infinite vertical permeable plate in the presence of magnetic field, heat generation or absorption, thermophoresis and Brownian diffusion effects. The analysis of MHD free convective flow of Al_2O_3 -water based nanofluid in an open cavity considering uniform thermal boundary condition in the presence of uniform heat absorption/generation was performed by Mahmoudi *et al*. [28].

In all the aforesaid studies, the solutions were analyzed by considering the simplified conditions, where velocity and temperature at the plate are continuous and defined. But, numerous problems of practical interest require the velocity and temperature to satisfy non-uniform, discontinuous or arbitrary conditions at the plate. Following this, several researchers, namely, Chandran *et al*. [29], Seth *et al*. [30-32], Nandkyeolyar *et al*. [33-34] and Hussain *et al*. [35] studied the problems of convective flow past a moving plate considering the ramped temperature. Khalid *et al*. [36] obtained the exact solution for natural convective flow of nanofluid past an oscillating moving vertical plate with ramped temperature, using the Laplace transform technique. Hussain *et al*. [37] explored the combined effects of Hall current and rotation on natural convective flow with heat transfer over an accelerated moving ramped temperature in the presence of heat absorption and homogenous chemical reaction employing the Laplace transform technique. Recently, Hussain *et al*. [38-39] discussed the impact of thermal radiation on the magneto free convective nanofluid over a moving uniformly accelerated ramped temperature plate with and without considering Hall effects into account. Subsequently, Sharma *et al*. [40] extended this problem in a rotating medium by making use of Laplace transform technique [42].

Objective of present research work is to analyze the consequence of heat absorption on the natural convective flow of incompressible, viscous and electrically conducting magneto-nanofluid over an impulsively moving ramped temperature plate. It is expected that the present findings will be useful in biological and physical sciences, transportation, electronics cooling, environment and national security.

2. MATHEMATICAL ANALYSIS

2.1 *Formulation of problem and its solution*

In the current work, we have taken into account an impulsively moving vertical infinite plate over an unstable hydromagnetic natural convective flow of an electrically conducting, viscous, and incompressible nanofluid. The coordinate system is chosen as the following: horizontal axis (x') is considered along the length of the plate in upward direction and vertical axis (y') is normal to the plane of plate. A uniform transverse magnetic field B_0 is applied in a direction which is parallel to y'-axis. The fluid and plate are at rest and maintain at a uniform temperature α'_∞ at time $t' \le 0$. At time $t' > 0$, the plate starts moving in x'-direction with uniform velocity U_0 in its own plane. The temperature of the plate is increased or lower to $\alpha'_\infty + (\alpha'_w - \alpha'_\infty) t'/t_0$ when $0 < t' \le t_0$ and it is maintained at invariant temperature α'_w when $t' > t_0$ (t_0 being characteristic time).

Fig. 1 displays the model's schematic diagram.

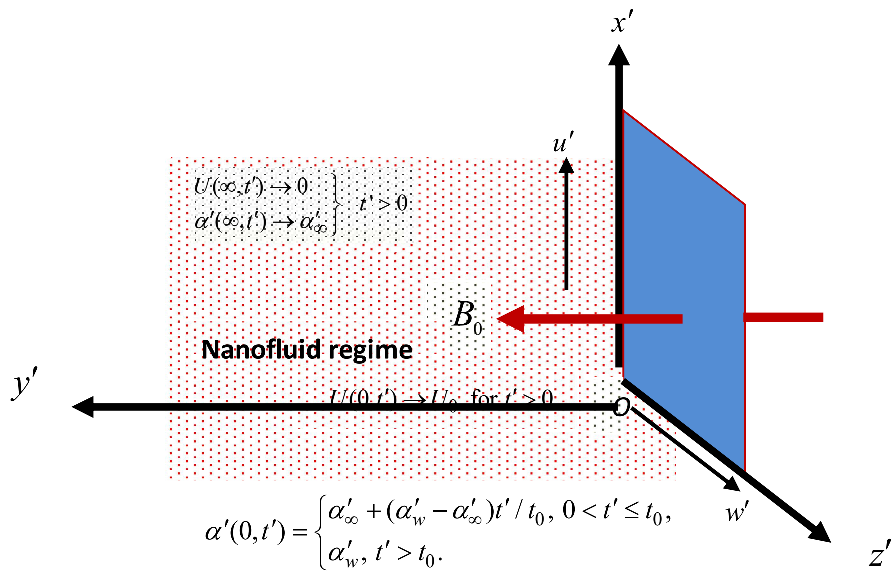

Fig. 1 The Geometric flowing diagram

The water based nanofluid is considered containing the three types of nanoparticles of Cu, Al_2O_3 and TiO_2. The nanoparticles are assumed to have uniform shape and size. Moreover, it is also assumed that both the base fluid and the nanoparticles are in thermal equilibrium state and no slip takes place between them. The thermo physical properties of base fluid and nanoparticles are given in Table 1. The plate is considered to be of infinite extent in x' and z' directions and is electrically non-conducting so all physical quantities except pressure is the functions of y' and t' only. Since the magnetic Reynolds number of the flow is taken to be very small, the induced magnetic field is neglected so that magnetic field $\vec{B} \equiv (0, B_0, 0)$. No electric field is applied, so the electric field due to polarization of charges is negligible; that is $\vec{E} \equiv (0,0,0)$. This corresponds to the case where no energy is added or extracted from the fluid by electrical means.

Table 1 Base fluid's thermos-physical characteristics and that of nanoparticles [42]

	Water (Base fluid)	**Cu (Copper)**	**Al_2O_3 (Alumina)**	**TiO_2 (Titanium Oxide)**
ρ: *density* $\left(\text{kg/m}^3\right)$	997.1	8933	3970	4250
c_p : *heat capacitance* $\left(\text{J/kg K}\right)$	4179	385	765	686.2
k :*ThermalConductivity* $\left(\text{W/m K}\right)$	0.613	401	40	8.9538
$\beta\times10^5$:*thermal expansion coefficient* $\left(K^{-1}\right)$	21	1.67	0.85	0.90
ϕ:*Volume Fraction*	0.00	0.05	0.15	0.20
σ:*Electrical Conductivity* $\left(\text{S/m}\right)$	5.5×10^{-6}	59.6×10^{6}	35×10^{6}	2.6×10^{6}

The governing equations for natural convective flow of an electrically conducting, viscous, and incompressible magneto-nanofluid accounting for the effects of heat absorption are given by using the aforementioned assumptions and the Boussinesq approximation.

$$\rho_{nf}\frac{\partial U}{\partial t'}=\mu_{nf}\frac{\partial^2 U}{\partial y'^2}-\sigma_{nf}B_0^2U+g\left(\rho\beta\right)_{nf}\left(\alpha'-\alpha'_\infty\right), \tag{1}$$

$$\frac{\partial\alpha'}{\partial t'}=\frac{k_{nf}}{\left(\rho c_p\right)_{nf}}\frac{\partial^2\alpha'}{\partial y'^2}-\frac{Q_0}{\left(\rho c_p\right)_{nf}}(\alpha'-\alpha'_\infty), \tag{2}$$

Initial and boundary conditions for the nanofluid flow problem are

$$\left.\begin{array}{l} U=0,\ \alpha'=\alpha'_\infty \text{ for } y'\geq 0 \text{ and } t'\leq 0,\\ U=U_0 \text{ at } y'=0 \text{ for } t'>0,\\ \alpha'=\alpha'_\infty+\left(\alpha'_w-\alpha'_\infty\right)t'/t_0 \text{ at } y'=0 \text{ for } 0<t'\leq t_0,\\ \alpha'=\alpha'_w \text{ at } y'=0 \text{ for } t'>t_0,\\ U\to 0,\ \alpha'\to\alpha'_\infty \text{ as } y'\to\infty \text{ for } t'>0. \end{array}\right\} \tag{3}$$

The expressions for ρ_{nf}, μ_{nf}, σ_{nf},$\left(\rho\beta\right)_{nf}$ and $\left(\rho c_p\right)_{nf}$ the nanofluids, are given as

$$\left.\begin{array}{l} \rho_{nf}=\left(1-\phi\right)\rho_f+\phi\rho_s,\ \mu_{nf}=\mu_f\left(1-\phi\right)^{-2.5},\\ \left(\rho\beta\right)_{nf}=\left(1-\phi\right)\left(\rho\beta\right)_f+\phi\left(\rho\beta\right)_s,\\ \left(\rho c_p\right)_{nf}=\left(1-\phi\right)\left(\rho c_p\right)_f+\phi\left(\rho c_p\right)_s,\\ \sigma_{nf}=\sigma_f\left[1+\dfrac{3\left(\sigma-1\right)\phi}{\left(\sigma+2\right)-\left(\sigma-1\right)\phi}\right],\ \sigma=\dfrac{\sigma_s}{\sigma_f}, \end{array}\right\} \tag{4}$$

The formulas given in equation (4) are only applicable to spherical nanoparticles; they are invalid for nanoparticles of other shapes. The Hamilton and Crosser model used by Oztop and Abu-Nada [38] for the effective thermal conductivity of the nanofluid, i.e. for the spherical nanoparticles, is represented as

$$k_{nf} = k_f \left[\frac{k_s + 2k_f - 2\phi\left(k_f - k_s\right)}{k_s + 2k_f + \phi\left(k_f - k_s\right)} \right], \tag{5}$$

Adding the following non-dimensional variables and parameters will allow equations (1) to (3) to be transformed into a dimensionless form:

$$y = \frac{y'}{U_0 t_0}, u = \frac{U}{U_0}, t = \frac{t'}{t_0}, \alpha = \frac{\alpha' - \alpha'_\infty}{\alpha'_w - \alpha'_\infty}. \tag{6}$$

Equations (1) and (2), in dimensionless form, reduce to

$$\frac{\partial u}{\partial t} = K_1 \frac{\partial^2 u}{\partial y^2} - K_2 M^2 u + K_3 G_r \alpha , \tag{7}$$

$$\frac{\partial \alpha}{\partial t} = \frac{1}{K_5} \frac{\partial^2 \alpha}{\partial y^2} - K_6 \alpha , \tag{8}$$

where,

$$\left.\begin{aligned}
&\lambda_1 = \left[(1-\phi) + \phi\left(\frac{\rho_s}{\rho_f}\right) \right], \quad \lambda_2 = \left[1 + \frac{3(\sigma-1)\phi}{(\sigma+2)-(\sigma-1)\phi} \right], \quad \sigma = \frac{\sigma_s}{\sigma_f}, \\
&\lambda_3 = \left[(1-\phi) + \phi\frac{(\rho\beta)_s}{(\rho\beta)_f} \right], \lambda_4 = \left[(1-\phi) + \phi\frac{(\rho c_p)_s}{(\rho c_p)_f} \right], Q = \frac{\upsilon_f Q_0}{(\rho c_p)_f U_0^2} \\
&K_1 = \frac{1}{(1-\phi)^{2.5}\lambda_1}, K_2 = \frac{\lambda_2}{\lambda_1}, \quad K_3 = \frac{\lambda_3}{\lambda_1}, \quad K_4 = \frac{k_{nf}}{k_f}, \quad K_5 = \frac{P_r}{K_4}, K_6 = \frac{Q}{\lambda_4} \\
&M = \frac{\sigma_f B_0^2 \upsilon_f}{\rho_f U_0^2}, G_r = \left[\frac{g\beta_f \upsilon_f (\alpha'_w - \alpha'_\infty)}{U_0^3} \right], \quad P_r = \frac{(\rho\upsilon c_p)_f}{k_f}.
\end{aligned}\right\} \tag{9}$$

According to the non-dimensional process discussed above, the characteristic time t_0 can be defined as $t_0 = \upsilon_f / U_0^2$, (U_0 is characteristic velocity).

The dimensionless form of the initial and boundary conditions (3) reduces

$$\left.\begin{aligned}
&u = 0, \ \alpha = 0 \ \text{ for } y \geq 0 \ \text{ and } t \leq 0, \\
&u = 1 \text{ at } y = 0 \ \text{ for } \ t > 0, \\
&\alpha = t \ \text{ at } \ y = 0 \ \text{ for } \ 0 < t \leq 1, \\
&\alpha = 1 \ \text{ at } \ y = 0 \ \text{ for } \ t > 1, \\
&u \to 0, \ \alpha \to 0 \ \text{ as } \ y \to \infty \text{ for } t > 0.
\end{aligned}\right\} \tag{10}$$

Catalyst Research Volume 23, Issue 2, September 2023 Pp. 1262-1278

With the use of the Laplace Transform technique, the equations (7) and (8) are analytically solved using the condition (10), and the solutions for nanofluid velocity and temperature are obtained as

$$u(y,t)=\frac{1}{2}g(y,t)+\lambda_3\left[f_1(y,t)-H(t-1)f_1(y,t-1)\right], \tag{11}$$

$$\alpha(y,t)=\alpha_1(y,t)-H(t-1)\ \alpha_1(y,t-1), \tag{12}$$

where,

$$g(y,t)=\left[e^{y\sqrt{\lambda_1\lambda_2}}erfc\left(\sqrt{\lambda_2 t}+\frac{y}{2}\sqrt{\frac{\lambda_1}{t}}\right)+e^{-y\sqrt{\lambda_1\lambda_2}}erfc\left(-\sqrt{\lambda_2 t}+\frac{y}{2}\sqrt{\frac{\lambda_1}{t}}\right)\right], \tag{13}$$

$$\alpha_1(y,t)=\frac{1}{2}\left[\left(t+\frac{y}{2}\sqrt{\frac{K_5}{K_6}}\right)e^{y\sqrt{K_5\ K_6}}erfc\left(\sqrt{K_6 t}+\frac{y}{2}\sqrt{\frac{K_5}{t}}\right)+\right.$$
$$\left.\left(t-\frac{y}{2}\sqrt{\frac{K_5}{K_6}}\right)e^{-y\sqrt{K_5\ K_6}}erfc\left(-\sqrt{K_6 t}+\frac{y}{2}\sqrt{\frac{K_5}{t}}\right)\right], \tag{14}$$

$$f_1(y,t)=\frac{e^{\lambda_4 t}}{2\lambda_4{}^2}\left[e^{y\sqrt{\lambda_1(\lambda_2+\lambda_4)}}erfc\left(\sqrt{(\lambda_2+\lambda_4)t}+\frac{y}{2}\sqrt{\frac{\lambda_1}{t}}\right)+e^{-y\sqrt{\lambda_1(\lambda_2+\lambda_4)}}erf\left(-\sqrt{(\lambda_2+\lambda_4)t}+\frac{y}{2}\sqrt{\frac{\lambda_1}{t}}\right)\right.$$
$$\left.-e^{y\sqrt{K_5(K_6+\lambda_4)}}erf(\sqrt{(K_6+\lambda_4)t}+\frac{y}{2}\sqrt{\frac{K_5}{t}}-e^{-y\sqrt{K_5(K_6+\lambda_4)}}erf(-\sqrt{(K_6+\lambda_4)t}+\frac{y}{2}\sqrt{\frac{K_5}{t}}\right]$$
$$-\frac{1}{2\lambda_4}\left[\left\{\frac{1}{\lambda_4}+\left(t+\frac{y}{2}\sqrt{\frac{\lambda_1}{\lambda_2}}\right)\right\}\left\{e^{y\sqrt{\lambda_1\lambda_2}}erf\left(\sqrt{\lambda_2 t}+\frac{y}{2}\sqrt{\frac{\lambda_1}{t}}\right)\right\}\right.$$
$$+\left\{\frac{1}{\lambda_4}+\left(t-\frac{y}{2}\sqrt{\frac{\lambda_1}{\lambda_2}}\right)\right\}\left\{e^{-y\sqrt{\lambda_1\lambda_2}}erf\left(-\sqrt{\lambda_2 t}+\frac{y}{2}\sqrt{\frac{\lambda_1}{t}}\right)\right\}$$
$$-\left\{\frac{1}{\lambda_4}+\left(t+\frac{y}{2}\sqrt{\frac{K_5}{K_6}}\right)\right\}\left\{e^{y\sqrt{K_5K_6}}erf\left(\sqrt{K_6 t}+\frac{y}{2}\sqrt{\frac{K_5}{t}}\right)\right\}$$
$$\left.-\left\{\frac{1}{\lambda_4}+\left(t-\frac{y}{2}\sqrt{\frac{K_5}{6K_2}}\right)\right\}\left\{e^{-y\sqrt{K_5K_6}}erf\left(-\sqrt{K_6 t}+\frac{y}{2}\sqrt{\frac{K_5}{t}}\right)\right\}\right]. \tag{15}$$

Here $H(t-1)$ and $erfc(x)$ are, respectively, Heaviside step and complementary error functions.

2.2 *Solution for the case of isothermal plate*

The solutions for the time-dependent natural convective flow of electrically conducting, viscous, and incompressible magneto-nanofluids over an impulsively moving vertical ramped temperature plate under the influence of heat absorption are represented by the expressions (11) to (15). It is worthwhile to contrast this flow with the one near a vertical, uniform temperature plate that is impulsively moving in order to examine the impact of ramping temperature on the flow-field. The solutions for the nanofluid velocity and temperature for naturally convecting magneto-nanofluids flow over an impulsively moving vertical plate with isothermal conditions are derived and are expressed in the following ways thanks to the assumptions made in the aforementioned section 2.1.

$$u(y,t)=\frac{1}{2}\left[e^{y\sqrt{\lambda_1\lambda_2}}erfc\left(\sqrt{\lambda_2 t}+\frac{y}{2}\sqrt{\frac{\lambda_1}{t}}\right)+e^{-y\sqrt{\lambda_1\lambda_2}}erfc\left(-\sqrt{\lambda_2 t}+\frac{y}{2}\sqrt{\frac{\lambda_1}{t}}\right)\right]$$

$$+\frac{\lambda_3}{\lambda_4}\left[\frac{e^{\lambda_4 t}}{2}\left\{e^{y\sqrt{\lambda_1(\lambda_2+\lambda_4)}}erfc\left(\sqrt{(\lambda_2+\lambda_4)t}+\frac{y}{2}\sqrt{\frac{\lambda_1}{t}}\right)+e^{-y\sqrt{\lambda_1(\lambda_2+\lambda_4)}}erfc\left(-\sqrt{(\lambda_2+\lambda_4)t}+\frac{y}{2}\sqrt{\frac{\lambda_1}{t}}\right)\right.\right.$$

$$\left.\left.-e^{y\sqrt{K_5(K_6+\lambda_4)}}erfc\left(\sqrt{(K_6+\lambda_4)t}+\frac{y}{2}\sqrt{\frac{K_5}{t}}\right)-e^{-y\sqrt{K_5(K_6+\lambda_4)}}erfc\left(-\sqrt{(K_6+\lambda_4)t}+\frac{y}{2}\sqrt{\frac{K_5}{t}}\right)\right\}\right]$$

$$-\frac{\lambda_3}{\lambda_4}\left[\frac{1}{2}\left\{e^{y\sqrt{\lambda_1\lambda_2}}erfc\left(\sqrt{\lambda_2 t}+\frac{y}{2}\sqrt{\frac{\lambda_1}{t}}\right)+e^{-y\sqrt{\lambda_1\lambda_2}}erfc\left(-\sqrt{\lambda_2 t}+\frac{y}{2}\sqrt{\frac{\lambda_1}{t}}\right)\right.\right.$$

$$\left.\left.-e^{y\sqrt{K_5K_6}}erfc\left(\sqrt{K_6 t}+\frac{y}{2}\sqrt{\frac{K_5}{t}}\right)+e^{-y\sqrt{K_5K_6}}erfc\left(-\sqrt{K_6 t}+\frac{y}{2}\sqrt{\frac{K_5}{t}}\right)\right\}\right], \qquad (16)$$

$$\alpha(y,t)=\frac{1}{2}\left[e^{y\sqrt{K_5K_6}}erfc\left(\sqrt{K_6 t}+\frac{y}{2}\sqrt{\frac{K_5}{t}}\right)+e^{-y\sqrt{K_5K_6}}erfc\left(-\sqrt{K_6 t}+\frac{y}{2}\sqrt{\frac{K_5}{t}}\right)\right]. \qquad 17)$$

2.3 ***Skin friction and Nusselt number***

The following expressions are given for both ramped and isothermal cases for N_u (Nusselt Number), which measures the rate of heat transfer at the plate, and τ (skin friction), which measures the shear stress at the plate:

For ramped temperature plate,

$$Nu=-\frac{1}{2}\left[\left(\sqrt{\frac{K_5}{K_6}}+2t\sqrt{K_5K_6}\right)\left\{erfc(\sqrt{K_6 t})-1\right\}-2\sqrt{\frac{K_5}{t\pi}}\,e^{-K_6 t}\right]$$

$$-\frac{1}{2}H(t-1)\left[\left(\sqrt{\frac{K_5}{K_6}}+2(t-1)\sqrt{K_5K_6}\right)\left\{erfc(\sqrt{K_6(t-1)})-1\right\}-2\sqrt{\frac{K_5}{(t-1)\pi}}\,e^{-K_6(t-1)}\right], \qquad (18)$$

$$\tau=\sqrt{a_1a_2}\left\{erfc(\sqrt{a_2 t})-1\right\}-\sqrt{\frac{a_1}{t\pi}}\,e^{-a_2 t}+a_3\left[f_2(t)-H(t-1)f_2(t-1)\right],$$

(19)

where,

$$f_2(t)=\frac{e^{a_4 t}}{a_4}\left[\sqrt{a_1(a_2+a_4)}\left\{erfc\left(\sqrt{(a_2+a_4)t}\right)-1\right\}-\sqrt{K_5(K_6+a_4)}\left\{erfc\left(\sqrt{(K_6+a_4)t}\right)-1\right\}\right.$$
$$\left.-\sqrt{\frac{a_1}{t\pi}}\,e^{-(\lambda_2+\lambda_4)t}+\sqrt{\frac{K_5}{t\pi}}\,e^{-(K_6+a_4)t}\right]$$
$$-\frac{1}{2a_4}\left[\sqrt{\frac{a_1}{a_2}}\left\{erfc\left(\sqrt{a_2 t}\right)-1\right\}+\left(\frac{1}{a_4}+t\right)\sqrt{a_1 a_2}\,2\left\{erfc\left(\sqrt{a_2 t}\right)-1\right\}-\left(\frac{1}{a_4}+t\right)\sqrt{\frac{a_1}{t\pi}}\,2e^{-a_2 t}\right.$$
$$\left.+\sqrt{\frac{K_5}{K_6}}\left\{erfc\left(\sqrt{K_6 t}\right)-1\right\}+\left(\frac{1}{a_4}+t\right)\sqrt{K_5 K_6}\,2\left\{erfc\left(\sqrt{K_6 t}\right)-1\right\}-\left(\frac{1}{a_4}+t\right)\sqrt{\frac{K_5}{t\pi}}\,2e^{-K_6 t}\right],$$
$$a_1=\frac{1}{K_1},\; a_2=MK_2,\; a_3=\frac{G_r\cdot a_1\cdot K_3}{K_5-a_1}\text{ and } a_4=\frac{K_5\cdot K_6+a_1\cdot a_2}{K_5-a_1}.$$

For isothermal temperature plate,

$$Nu=\sqrt{\frac{K_5}{t\pi}}\,e^{-K_6 t}-\sqrt{K_5 K_6}\left\{erfc(\sqrt{K_6 t})-1\right\}, \tag{20}$$

$$\tau=\left[\sqrt{a_1 a_2}\left\{erfc\left(\sqrt{a_2 t}\right)-1\right\}-\sqrt{\frac{a_1}{t\pi}}\,e^{-a_2 t}\right]+\frac{a_3}{a_4}\left[e^{a_4 t}\left\{\sqrt{a_1(a_2+a_4)}\left\{erfc\left(\sqrt{(a_2+a_4)t}\right)-1\right\}\right.\right.$$
$$\left.\left.-\sqrt{\frac{a_1}{t\pi}}\,e^{-(a_2+a_4)t}-\sqrt{K_5(K_6+a_4)}\left\{erfc\left(\sqrt{(K_6+a_4)t}\right)-1\right\}-\sqrt{\frac{K_5}{t\pi}}\,e^{-(K_6+a_4)t}\right\}\right]$$
$$-\frac{a_3}{a_4}\left[\sqrt{a_1 a_2}\left\{erfc\left(\sqrt{a_2 t}\right)-1\right\}-\sqrt{\frac{a_1}{t\pi}}\,e^{-a_2 t}-\sqrt{K_5 K_6}\left\{erfc\left(\sqrt{K_6 t}\right)-1\right\}+\sqrt{\frac{K_5}{t\pi}}\,e^{-K_6 t}\right]. \tag{21}$$

3. RESULTS AND DISCUSSION

The numerical results for the nanofluid velocity and temperature are discussed with the help of several graphs in order to highlight the influence of different physical parameters on the flow-fluid. The numerical values of skin friction and the Nusselt number have been described by many tables for engineering purposes. Three distinct types of water-based nanofluids with the nanoparticles of Cu (copper), Al_2O_3 (aluminium oxide) and TiO_2 (titanium oxide) have been taken into account. The numerical values of Cu-water based nanofluid velocity $u(y,t)$, computed from the analytical solutions reported in sections 2.1 and 2.2 have been shown by many graphs against the boundary layer coordinate y in Figs. 2-6 for several values of M, Q, G_r, ϕ and t taking $P_r=6.2$. The values of ϕ are considered in the range $0.05<\phi\le 0.25$. In addition, the spherical nanoparticles with thermal conductivity and their dynamic viscosity are mentioned in Table 1. The values of other physical parameters have been shown in the depiction of respective figures. It can be observed from Figs. 2 and 3, that the nanofluid velocity gets reduced due to reduce in magnetic and heat absorption parameters *M* and Q respectively. This may be endorsed to the fact that, the existence of magnetic field in the presence of an electrically conducting nanofluid generates a resistive type body force, termed as Lorentz force which has tendency to impede the motion of fluid in the boundary layer region. Fig. 4 shows that augmentation in G_r results the significant rise in the nanofluid velocity which is persistent to the fact that, the G_r behaves as a gratifying pressure gradient which accelerate the nanofluid velocity in the entire boundary layer region.

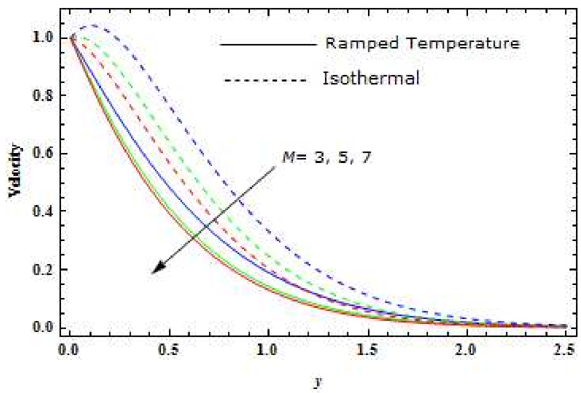

Fig. 2 Effect of *M* on velocity profiles.

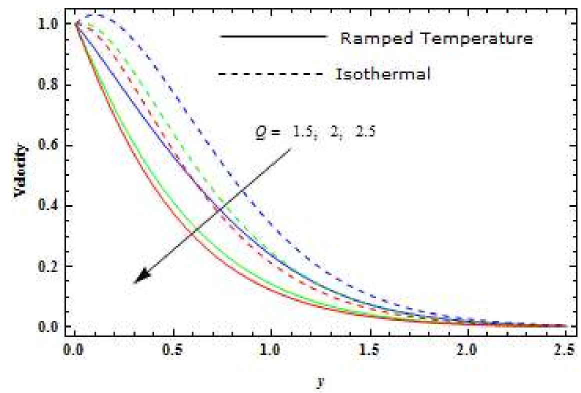

Fig. 3 Effect of Q on velocity profiles.

As demonstrated in Fig. 5, the nanofluid velocity is slowed down close to the plate while having an annulation effect farther away from the moving plate. This happens due to the reason that the increasing value of volume fraction of nanoparticle reduces the thermal conductivity of fluid which in turn the causes the thickness of boundary layer to reduce and the viscosity to increase thereby reducing the nanofluid velocity in the proximity of moving plate. Fig. 6 reveals that, as time passes the fluid velocity gets accelerated. The consequences of heat absorption parameter Q, nanoparticle volume fraction ϕ and time *t* on copper-water based temperature profiles are shown in Figs. 7-9, taking Prandtl number $P_r = 6.2$. From Fig. 7, it is observed that, as heat absorption parameter gradually increases, results the significant reduction in the nanofluid temperature for both the ramped and isothermal conditions. From Figs. 8-9, it is evident that the nanofluid temperature rises for the increase of nanoparticle volume fraction ϕ and time *t* for both the cases of ramped and isothermal conditions. Physically, it is described as the nanoparticles volume fraction have tendency to raise the nanofluid temperature throughout the boundary layer region, also nanofluid temperature gets augmented with the progress of time for both ramped and isothermal cases.

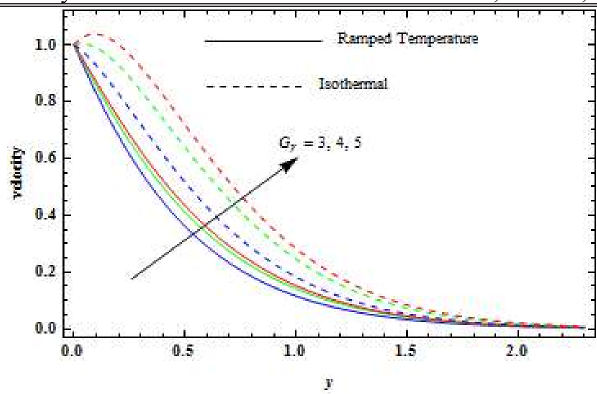

Fig. 4 Effect of G_r on velocity profiles.

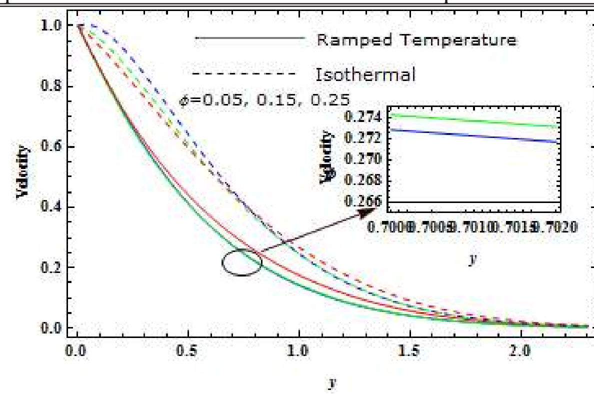

Fig. 5 Effect of ϕ on velocity profiles.

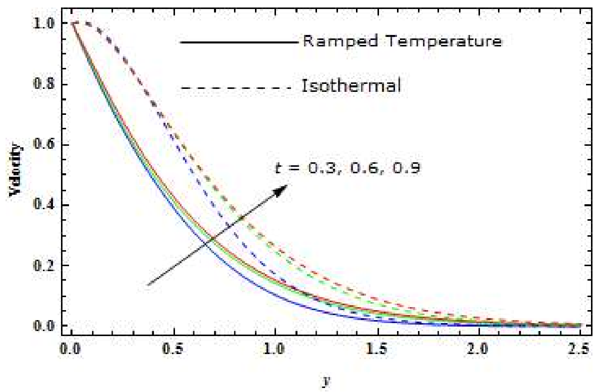

Fig. 6 Effect of *t* on velocity profiles.

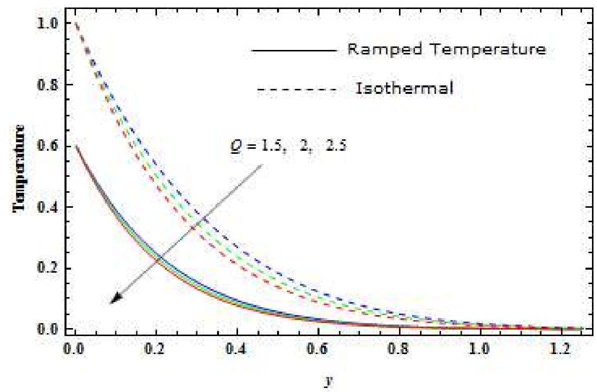

Fig. 7 Effect of Q on temperature profiles.

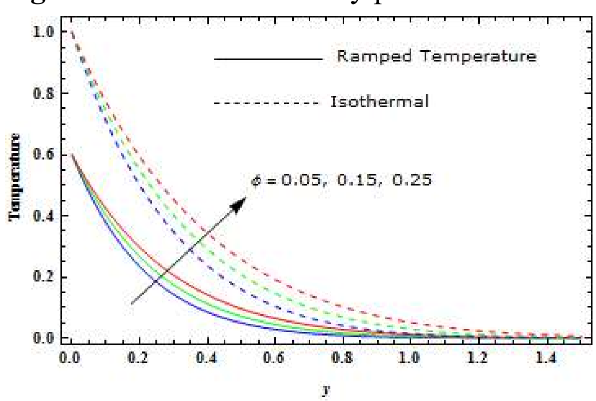

Fig. 8 Effect of ϕ on velocity profiles.

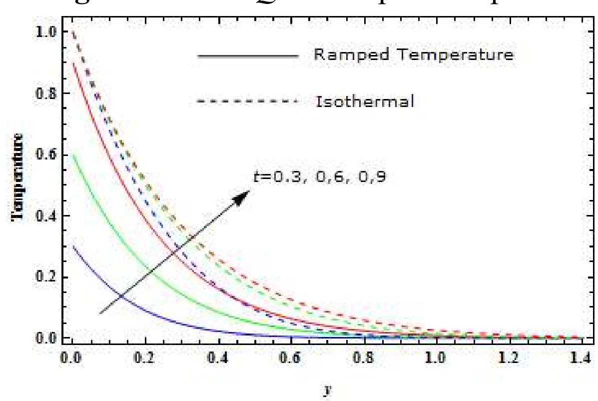

Fig. 9 Effect of *t* on temperature profiles.

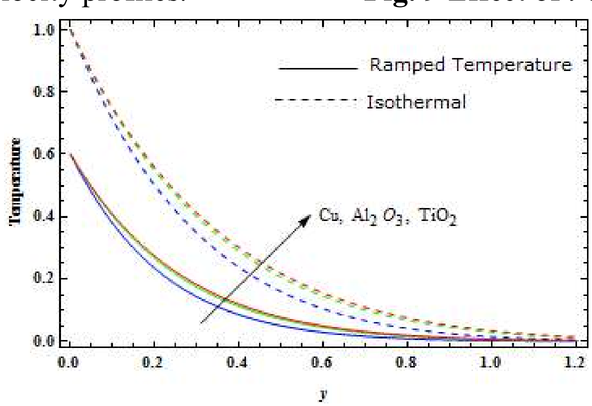

Catalyst Research Volume 23, Issue 2, September 2023 Pp. 1262-1278

Fig. 10 Comparison of temperature profiles for different nanofluids.

The comparison of nanofluid temperature profiles in the case of isothermal and ramped conditions for different nanofluids with the nanoparticles of Cu, Al_2O_3 and TiO_2 is depicted in Fig. 10. It is noticed from Fig. 10 that, for both isothermal and ramped conditions, the temperature of TiO_2 -water based nanofluid are higher in magnitude followed by the temperature of Al_2O_3-water and Cu-water based nanofluids.

The numerical values of skin friction τ for both cases of ramped and isothermal temperature plates considering the copper-water based nanofluid, evaluated from equations (19) and (21) are mentioned in Table 2 for the different values of M, G_r, ϕ, Q and t keeping Prandtl number $P_r = 6.2$. It is found from the Table 2 that, the shear stress increases due to increase of M, G_r, ϕ, Q and t. This infers that magnetic field, thermal buoyancy force, volume fraction of nanoparticle, heat absorption parameter have tendency to increase the shear stress at the plate, also it gets augmented as time passes for both the cases of ramped and isothermal. It is reckoned from Table 3 that, the Nusselt number Nu for both the cases of ramped and isothermal conditions, increases for increasing value of Q and it decreases with the increase of ϕ, whereas for the ramped case it increases and it decreases for isothermal case with the increase in t. This suggests that for both the case of ramped and isothermal, the rate of heat transfer at the plate gets raised with the augmentation of heat absorption parameter whereas volume fraction of nanoparticle has adverse effect on it. As time passes the rate of heat transfer gets improved for ramped case where as it gets reduced for isothermal case.

Table 2 Skin friction τ for Copper-water based nanofluid when $P_r = 6.2$

M	G_r	ϕ	Q	t	τ (ramped temp.)	τ (isothermal temp.)
3					6.15463	5.80615
5	4				6.29641	6.14205
7		0.5			6.58365	6.58457
	3				4.99342	4.82386
	4		2		6.29641	6.14205
	5				7.59940	7.46024
		0.05		0.6	6.29641	6.14205
		0.15			9.81332	9.37154
		0.25			19.1638	18.7232
5	4		**1.5**		4.32815	4.35649
		0.5	**2**		6.29641	6.14205
			2.5		8.98351	8.71207
			2	**0.3**	3.52347	2.84424

				0.6	6.29641	6.14205
				0.9	17.8309	17.7829

Table 3 Nusselt number N_u for Copper-water based nanofluid

ϕ	Q	t	N_u (ramped temp.)	N_u (isothermal temp.)
0.05	2	0.6	2.94341	3.38195
0.15			2.54640	2.94062
0.25			2.21385	2.56973
0.5	**1.5**		2.84580	3.00798
	2		2.94341	3.38195
	2.5		3.05186	3.72975
	2	**0.3**	2.60289	3.68166
		0.6	2.94341	3.38195
		0.9	3.76742	3.31097

4. STATISTICAL ANALYSIS: ESTIMATION OF SKIN FRICTION τ AND NUSSELT NUMBER N_u

Here, we have used the multiple quadratic regression analysis [43] to estimate the relationship between two or more variables. Here, quadratic regression estimation analysis for skin friction coefficients and Nusselt number are presented. The model of multiple quadratic regression estimation for coefficient of skin friction is mentioned for 100 different values of M and Q, obtained arbitrarily from intervals [1, 7] and [0.5, 2.5] respectively for two different values of ϕ = 0.05 and ϕ = 0.15. Apart from this, a model of multiple quadratic regression estimation for Nusselt number is provided for 100 different values of Q and t, analyzed arbitrarily from intervals [1, 7] and [0.3, 0.9] for two different values of ϕ = 0.05 and ϕ = 0.15.

The estimated quadratic regression model for τ corresponding to M and Q, is given as follows:

$$\tau_{est} = \tau + b_1 M + b_2 Q + b_3 M^2 + b_4 Q^2 + b_5 MQ.$$

and regression model for ***Nu*** corresponding to Q and t, is given as

$$Nu_{est} = Nu + c_1 Q + c_2 t + c_3 Q^2 + c_4 t^2 + c_5 Qt.$$

The maximum relative error bound are

for skin friction i.e., $\varepsilon_\tau = \dfrac{|\tau_{est} - \tau|}{\tau}$ and

for Nusselt number i.e., $\varepsilon_{Nu} = \dfrac{|Nu_{est} - Nu|}{Nu}$

Table 4 Values of error bound ε_τ and regression coefficients for estimated τ (variations in M and Q).

ϕ	τ	b_1	b_2	b_3	b_4	b_5	ε_τ
0.05	6.29641	0.2181	0.0179	0.1304	0.0103	0.0078	0.0053
0.15	9.81332	0.2083	0.0162	0.1002	0.0097	0.0062	0.0037

Table 5 Values of error bound ε_{Nu} and regression coefficients for estimated τ (variations in Q and T).

ϕ	N_u	c_1	c_2	c_3	c_4	c_5	ε_{Nu}
0.05	2.94341	1.2001	0.9871	0.7689	0.4539	0.0187	0.00087
0.15	2.54640	1.2098	0.8732	0.6530	0.4162	0.0136	0.00076

Tables 4 and 5 shows the coefficients of multiple quadratic regression estimated values of skin friction coefficients and Nusselt number corresponding to different parameters. From the tabulated data, we found that heat absorption parameter Q is higher than that of magnetic field parameter. This suggests that the variation in skin friction coefficient is more sensitive Q than that of M for both values of ϕ. Correspondingly, we can observe that the Nusselt number is more prone to heat absorption parameter Q when time elapsed.

5. VALIDATION OF OBTAINED RESULTS

The obtained results of the present paper have been validated by comparing the nanofluid velocity profiles with the results obtained by Khalid et al. [36] considering the similar assumptions without Magnetic field and heat absorption. This comparison shows an excellent conformity of our results as it is revealed from Fig. 11.

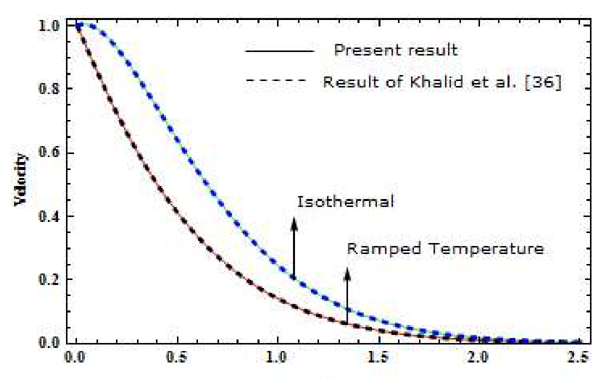

Fig. 11 Comparison of velocity profiles of present result considering $M = Q = 0$ with those obtained by Khalid *et al*. [36] when $\omega = 0$.

6. CONCLUSIONS

By using the Laplace transform technique to examine the effects of different parameters on the natural convective electrically conducting viscous magneto-nanofluid over an impulsively moving ramped temperature plate. The key conclusions for both the scenarios of ramping temperature and isothermal plates are outlined below:

(i) When a magnetic field and an electrically conducting nanofluid are present, a resistive type body force is created, which has the potential to obstruct fluid mobility in the boundary layer region. The thermal buoyancy force behaves as a gratifying pressure gradient which accelerates nanofluid velocity in the regime of boundary layer.

(ii) As the volume fraction of nanoparticles grows, the thermal conductivity of the fluid decreases, reducing the thickness of the boundary layer and increasing the fluid's viscosity, which limits the velocity of the nanofluid near moving plates. As time goes on, the velocity of the nanofluid increases.

(iii) Heat absorption tends to lower the temperature of nanofluids, whilst the volume fraction of nanoparticles tends to raise them. The temperature of the nanofluid rises over time.

(iv) The shear stress of the plate is likely to grow as a result of the magnetic field, thermal buoyancy force, volume fraction of nanoparticles, and heat absorption parameter.

(v) While the volume fraction of nanoparticles has a negative impact on it, the rate of heat transfers at the plate increases with the increase in the heat absorption parameter. For the ramped scenario, the rate of heat transfer increases with time, but for the isothermal case, it decreases.

REFERENCES

[1] S.U.S. Choi, *ASME FED 231/MD*, 66, 99 (1995).
[2] P. Keblinski, S.R. Phillpot, S.U.S. Choi and J.A. Eastman, *Int. J. Heat Mass Transf.*, 42, 855 (2002).
[3] J. Buongiorno, *J. Heat Transf.*, 128, 240 (2006).
[4] S.P. Jang and S.U.S. Choi, *J. Heat Transf.*, 129, 617 (2007)
[5] W. Daungthongsuk and S. Wongwises, *Rene. & Sust. Energy Reviews*, 11, 797 (2007).
[6] S.M. Seyyedi, H. Bararnia, D.D. Ganji, M. Gorji-Bandpy and S. Soleimani, *Int. J. Thermal Sci.*, 61, 1(2012).
[7] M.M. Rashidi, E. Momoniat, M. Ferdows and A. Basiriparsa, *Math. Prob. Engg.*, (Article ID 239082) (2014).
[8] F. Garoosi, G. Bagheri and M.M. Rashidi, *Powder Tech.*, 275, 239 (2015).
[9] F. Garoosi, B. Rohani and M.M. Rashidi, Powder *Tech.*, 275, 304 (2015).
[10] A. Malvandi and D.D. Ganji, *Adv. Powder Tech.*, 25,1369 (2014).
[11] A. Malvandi and D.D. Ganji, *Particuology*, 24, 113 (2016).
[12] M. Sheikholeslami, M. Hatami and D.D. Ganji, *Powder Tech.*, 246, 327 (2013).
[13] M. Sheikholeslami, M. Gorji-Bandpy, R. Ellahi and A. Zeeshan, *J. Magnetism Magnetic Materials*, 369, 69 (2014).

[14] M. Sheikholeslami, M. Gorji-Bandpy and D.D. Ganji, *J. Taiwan Inst. Chem. Engineers*, 45, 1204 (2014).

[15] M. Sheikholeslami and D.D. Ganji, *Scientia Iranica B*, 21(1), 203 (2014).

[16] T. Hayat, T. Muhammad, A. Qayyum, A. Alsaedi and M. Mustafa, *J. Molecular Liquids*, 213, 179 (2016).

[17] R. Dhanai, P. Rana and L. Kumar, *Powder Tech*., 288, 140 (2016).

[18] S. Acharya and R.J. Goldstein, *J. Heat Transf.*, 107, 855 (1985).

[19] K. Vajravelu, J. Nayfeh, *Int. Commun. Heat Mass Transf.*, 19, 701 (1992).

[20] A.J. Chamkha, *Numer. Heat Transf.*, 32, 853 (1997).

[21] J.K. Leea, J. Koob, H. Hongb and Y.T. Kangb, *Int. J. Refrigeration*, 33, 269 (2010).

[22] M. Sheikh and Z. Abbas, *J. Magnetism and Magnetic Materials*, 396, 204 (2015).

[23] A. Mehmood and M. Saleem Iqbal, *J. Molecular Liq.*, 224, 1326 (2016).

[24] H. Mondal, P. De, S. Chatterjee, P. Sibanda and P.K. Roy, *J. Nanofluids*, 6, 189 (2017).

[25] R. Nandkeolyar, P.K. Kameswaran, S. Shaw and P. Sibanda, *J. Heat Transf.*, 136(12), 122001 (2014).

[26] M.A.A. Hamad and I. Pop, *Heat Mass Transf.*, 47, 1517 (2011).

[27] A.J. Chamkha and A.M. Aly, *Chem. Eng. Comm.*, 198, 425 (2011).

[28] A. Mahmoudi, I. Mejri, M.A. Abbassi and A. Omri, *Powder Tech.*, 269, 275 (2015).

[29] P. Chandran, N.C. Sacheeti, and A.K. Singh, *Heat Mass Transf.*, 41, 459 (2005).

[30] G.S. Seth, M.S. Ansari and R. Nandkeolyar, *Heat Mass transf.*, 47, 551 (2011).

[31] G.S. Seth, S.M. Hussain and S. Sarkar, *J. Porous Media*, 17(1), 67 (2014).

[32] G.S. Seth, S. Sarkar, S.M. Hussain and G.K. Mahato, *J. Appl. Fluid Mech.*, 8(1), 159 (2015).

[33] R. Nandkeolyar, G.S. Seth, O.D, Makinde, P. Sibanda and M.S. Ansari, *ASME J. Appl. Mech.*, 80, 061003 (2013).

[34] R. Nandkeolyar, M. Das and H. Pattnayak, *J. Orissa Mathematical Soc.*, 32, 15 (2013).

[35] S.M. Hussain, J. Jain and G.S. Seth, *Bul. Chem. Comm.,* 48(4), 659 (2016).

[36] A. Khalid, I. Khan and S. Shafie, *The Europ. Physical J. – Plus*, 130, 57 (2015).

[37] S.M. Hussain, J. Jain, G.S. Seth and M.M. Rashidi, *J. Magnetism Magnetic Materials*, 422, 112 (2017).

[38] S.M. Hussain, R. Sharma, M.K. Mishra and G. S. Seth, *J. Nanofluid*, 6(5), 840 (2017).

[39] S.M. Hussain, J. Jain, G.S. Seth, M.M. Rashidi, *Scientia Iranica B*, 25(3), 1243 (2018).

[40] R. Sharma, S.M. Hussain, H. Joshi and G.S. Seth, *Diffusion Foundations*, 11, 129 (2017).

[41] H.F. Oztop and E. Abu-Nada, Int. J. Heat Fluid Flow, 29(5), 1326 (2008).

[42] M. R. Mishra, S. M. Hussain, R. Sharma, G. S. Seth, Bulgarian Chemical Communications, 50(4), 621 (2018)

[43] S. M. Hussain, R. Sharma, M. R. Mishra, and S S. Alrashidy, Mathematics, 8 (2020)